Mode-selective electron-phonon coupling in laser photoemission on Cu(110)

Emi Minamitani,[1,*] Ryuichi Arafune,[2,†] Mayuko Q. Yamamoto,[3] Noriaki Takagi,[3] Maki Kawai,[3] and Yousoo Kim[1]

[1]*Surface and Interface Science Laboratory, RIKEN, 2-1 Hirosawa, Saitama 351-0198, Japan*

[2]*International Center for Materials Nanoarchitectonics, National Institute for Materials Sciences*

[3]*Department of Advanced Materials Science, The University of Tokyo, 5-1-5 Kashiwanoha, Kashiwa, Chiba 277-8561, Japan*

(Received 16 June 2013; revised manuscript received 19 November 2013; published 6 December 2013)

By combining density functional perturbation theory (DFPT) calculations and laser photoemission spectroscopy (LPES) experiments, we have clarified the selective coupling between low-energy photoelectrons and subsurface phonon modes. A step structure resulting from the inelastic scattering of photoelectrons appeared at 14.7 meV below the Fermi level in the LPES of Cu(110). We found that the inelastic step originates from an indirect excitation in which the electron is excited by the low-energy photon near the $\bar{Y}$ point and then scattered to the $\bar{\Gamma}$ point by phonon modes that are predominantly present in the subsurface region.

DOI: 10.1103/PhysRevB.88.224301 PACS number(s): 79.60.Bm, 63.20.D−, 68.35.Ja, 71.15.Mb

With improvements in energy resolution[1] of photoemission spectroscopy, which is one of the most reliable tools for determining electronic band structures,[2] several signals originating from the electron-phonon interactions have appeared in the spectrum apart from the vibrational progression structure in gas-phase experiments.[3] Two well-known examples are the "kink" structure around the Fermi wave number in the electronic band dispersion of metallic and superconducting systems determined with angle resolved photoemission experiments[4–6] and the linewidth broadening of the noble metal surface states as a function of temperature.[7,8] Both of them have been described by the electron self-energy attributable to the electron-phonon coupling around the Fermi level (E_F).[9–11]

Recently, a completely different manifestation of electron-phonon coupling, inelastically scattered photoelectron by phonons, was observed in low-energy photoemission spectra. One of us (R.A.) reported on a spectral component resulting from the inelastic scattering of the photoelectron with surface adsorbate vibrations[12] as well as phonons of solids.[13] Figure 1(a) shows laser photoemission spectroscopy (LPES) results of Cu(110),[14] which are discussed in this paper in detail. In addition to the Fermi-Dirac distribution curve originating from the elastic process, a single step structure appeared at 14.7 meV below E_F, which implies that the detected photoelectrons lose their energy through coupling with particular phonon modes. To highlight this step structure, the first derivative spectrum excited by 4.571 eV photon is shown in the bottom panel of Fig. 1(a). This step structure is a replica of the elastic component, which is downshifted by the energy of the phonon interacting with the photoelectron. Similar inelastic-scattering-induced structures were observed in the low-energy photoemission spectra of diamond.[15,16]

In the previous report,[13] we concluded that the photoelectron emitted from Cu(110) by the laser light did not interact with surface phonon, and we conjectured the mechanism of the inelastic interaction between the photoelectron and the phonon based on the bulk electron and phonon dispersion. This presumption explained the experimental observations to some extent; however, several points, in particular, why only the particular phonon modes couple with the photoelectron, were left unsolved. In order to explore the further possibility of detecting phonons by using LPES, more detailed and complete theoretical analysis has been seriously required. In our experiment, the photoelectrons were emitted from the $\bar{\Gamma}$ point in the surface Brillouin zone (SBZ), because photoemission spectra were measured in the normal-emission geometry. Therefore, the inelastic photoemission process is expected to be an indirect excitation process in which electrons of wave vector q couple with phonons of the same wave vector and scatter to the $\bar{\Gamma}$ point, as shown schematically in Fig. 1(c). In this paper, we investigate this indirect excitation process using *ab initio* calculations which includes electron-phonon coupling calculations based on the density functional perturbation theory[17] (DFPT).

Figure 1(b) shows the calculated electronic band dispersion of the 13-layer Cu(110) slab.[18] The surface states with the characteristic parabolic dispersion appear at the $\bar{Y}$ point in the SBZ. The position of the occupied surface states (approximately −0.5 eV from E_F) agrees with the results of previous DFT calculations[19] and angle-resolved photoemission spectroscopy experiments.[20] These results justify the selection of a 13-layer slab is an appropriate model system. The work function evaluated from the macroscopic average of the electrostatic potential[21] is 4.22 eV, which is lower than the experimental value (4.52 eV).[22] Generally, underestimation of the work function in slab models can be compensated for by referring to the potential and the Fermi energy of the bulk.[23] However, a recent investigation showed that using the bulk reference method for relaxed slabs can sometimes lead to poorer results.[24] Thus, we applied the value obtained directly from the slab calculation results. Figure 1(d) shows the phonon energy dispersion obtained using the same setup. The overall spectral shape reproduces both the characteristic surface and bulk phonon modes which are consistent with the DFT calculations and experimental results reported in the literature.[25,26] As shown in Fig. 1(d), there are no distinctive modes around 14.7 meV, which implies that inspecting the band structures alone is not sufficient for identifying phonon excitation at 14.7 meV and that calculating the electron-phonon coupling for the whole of modes is necessary.

Within the framework of perturbation theory, the lowest order process of the indirect excitation in LPES is that the electron in the initial state, wave vector $k = q$ and band

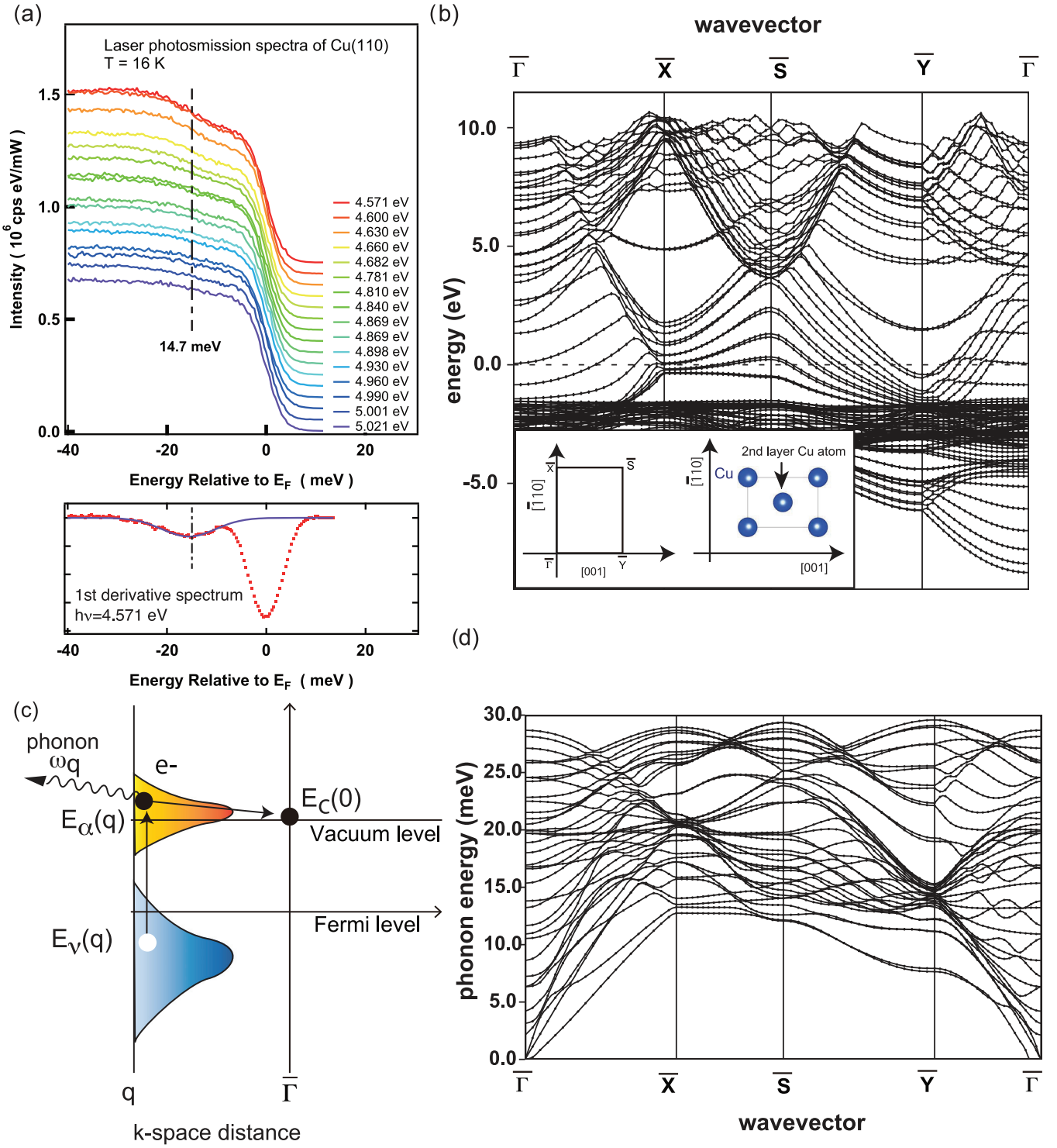

FIG. 1. (Color online) (a) (Top) LPES of the clean Cu(110) surface excited by the laser photon from 4.571 to 5.021 eV. The sample temperature is 16 K. The inelastic component is evaluated by deconvoluting the spectrum into two individual Fermi-Dirac distribution functions. The center of the Fermi-Dirac distribution function of the inelastic component is 14.7 meV below E_F, and the intensity of the inelastic component depends on the laser energy. (Bottom) First derivative spectrum excited by 4.571 eV photon. The curve has been smoothed to decrease the noise level in the derivative spectrum. (b) Calculated electronic band structure of Cu(110). A Shockley-type surface state appears around the $\bar{Y}$ point near E_F. Insets are the top view of the slab model and surface Brillouin zone of Cu(110), respectively. (c) Schematic diagram of the indirect excitation in LPES. (d) Calculated phonon band structure of Cu (110).

index v, is scattered to the final state, $k = 0$ and band index c, through the absorption of the single laser photon and emission of the single phonon. Under the dipole approximation, the perturbation from the external electromagnetic field

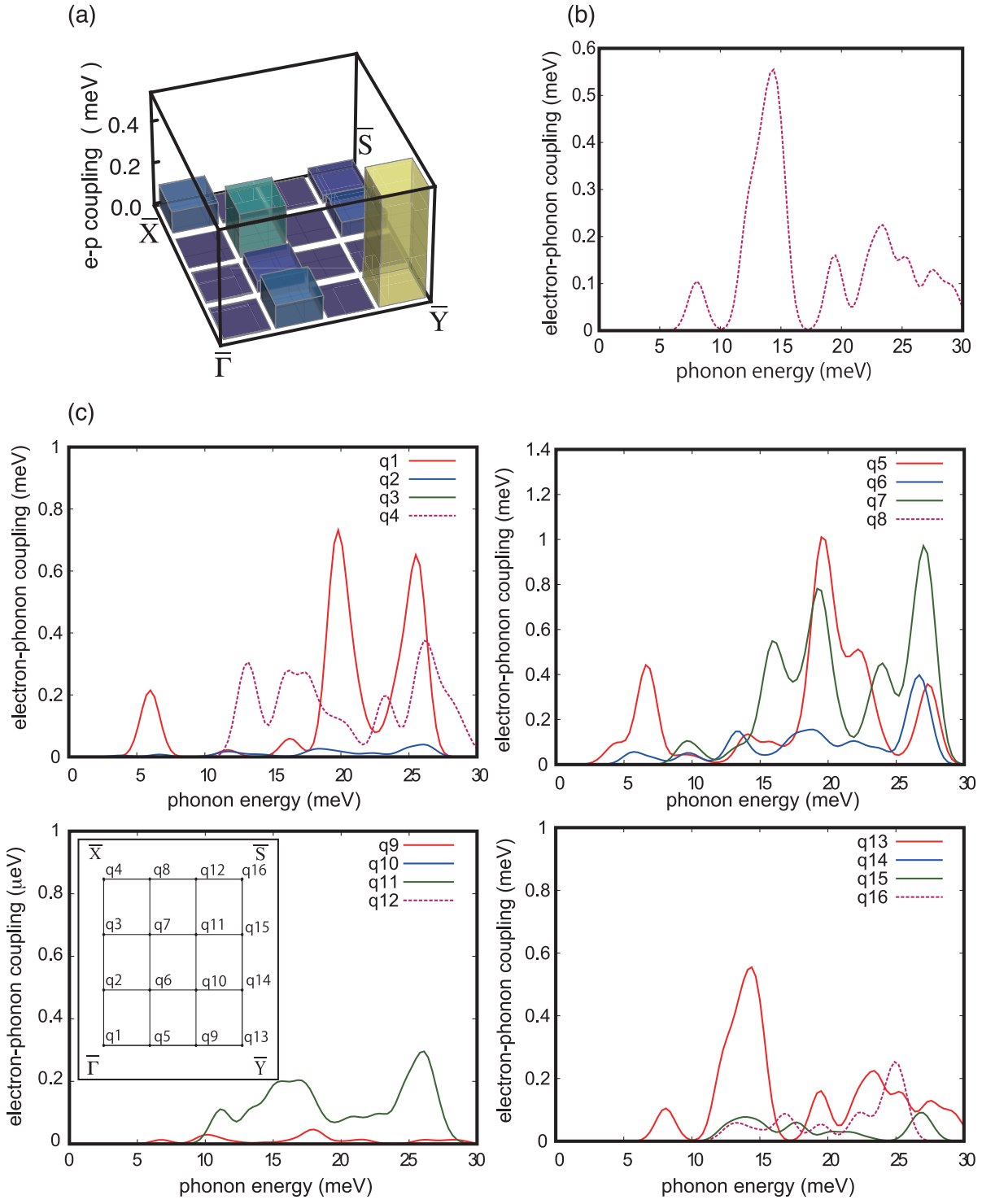

FIG. 2. (Color online) (a) Calculated electron-phonon coupling matrix element $\langle\psi_{0c}|V_p(q,i,r)|\psi_{q\alpha}\rangle$ with a phonon energy of 14.7 meV, which induces photoelectron scattering from the k point with wave vector q to the $\bar{\Gamma}$ point. To reproduce the low-energy photoelectron, we use the energy of E_V as the energy of photoelectron. The k point is sampled at 16 irreducible points in a $6 \times 6 \times 1$ mesh of the first Brillouin zone. In order to extract the contribution from the electronic state near E_V, we multiply $\delta(E_\alpha - E_v)$ which is approximated by the Gaussian function of $\sqrt{2\ln(2)} \times 50$ meV half width at half maximum (HWHM). Original discrete matrix elements are smeared by using the Gaussian function of $\sqrt{2\ln(2)}$ meV HWHM to treat electron-phonon coupling as a function of phonon energy. (b) Electron-phonon coupling spectrum at the $\bar{Y}$ point as a function of the phonon energy. The spectrum shows a main peak around 15 meV phonon energy, which describes well the single inelastic step structure in the LPES on Cu(110). (c) Calculated electron-phonon coupling at E_V as a function of the phonon energy that scatters the photoelectron from each k point to the $\bar{\Gamma}$ point. The calculation results include the contribution from the whole modes that exist at each k point. The k point is sampled at 16 irreducible points (labeled q1–q16) in a $6 \times 6 \times 1$ mesh of the first Brillouin zone. The inset shows the coordination of irreducible points in the surface Brillouin zone.

of frequency ω can be written as

$$H_{em}(r,t) = \frac{eA_0}{mc}\vec{e}\cdot\vec{p}e^{-i\omega t} + \text{H.c.} \quad (1)$$

Here, $\vec{e}$ is the polarization vector of the incident photon. The perturbation from the electron-phonon interaction can be written as

$$H_{ep}(r,t) = \frac{1}{\sqrt{N}}\sum_{q,i}^{B.Z.} V_p(q,i,r)e^{-i\omega_{qi}t}a_{qi} + \text{H.c.} \quad (2)$$

Here, a_{qi} is the annihilation operator of the phonon with the wave vector q, mode index i and frequency ω_{qi}. $\sum_{q,i}^{B.Z.}$ denotes the summation over all wave vectors and mode indexes in the first Brillouin zone. $V_p(q,i,r)$ is the perturbation of the electron-core potential that results from the displacement of the ion position by the phonon mode. The second order transition amplitude from these terms is given by[27]

$$T_{0c\leftarrow qv} = \frac{eA_0}{mc}\sqrt{n_q+1}\frac{1}{\sqrt{N}} \times\left\{\sum_{\alpha,i}\frac{\langle\psi_{0c}|V_p(q,i,r)|\psi_{q\alpha}\rangle\langle\psi_{q\alpha}|\vec{e}\cdot\vec{p}|\psi_{qv}\rangle}{E_v(q)-E_\alpha(q)+\hbar\omega} + \sum_{\beta,i}\frac{\langle\psi_{0c}|\vec{e}\cdot\vec{p}|\psi_{0\beta}\rangle\langle\psi_{0\beta}|V_p(q,i,r)|\psi_{qv}\rangle}{E_v(q)-E_\beta(0)+\hbar\omega_{qi}}\right\}. \quad (3)$$

Here, n_q is the occupation number of the phonon of wave vector q. $E_v(q)$ and $E_\alpha(q)$ [$E_\beta(0)$] are the energies of the initial and intermediate states, respectively. The first term represents an indirect excitation in which an electron is excited through the absorption of a single photon, and then scattered to the $\bar{\Gamma}$ point by a phonon emission. The second term represents the process that proceeds in the opposite order. As shown in Fig. 1(a), the height of the inelastic component depends on the excitation photon energy, whereas the height of the elastic component is essentially independent. The first term obviously describes the inelastic process that depends on the photon energy. The second term also involves the photon energy dependence essentially, because the transition matrix element $\langle\psi_{0c}|\vec{e}\cdot\vec{p}|\psi_{0\beta}\rangle$ which represents the photoexcitation at the $\bar{\Gamma}$ point is contained. However, the extremely weak dependence of the elastic component on the photon energy implies that the second term does not strongly depend on the photon energies within the measured range. Thus, we ascribe the main contribution of the indirect excitation to the first term in Eq. (3), which we focus on in the following discussion.

One of the governing parameters in the second term is the electron-phonon coupling matrix element, $\langle\psi_{0c}|V_p(q,i,r)|\psi_{q\alpha}\rangle$. Figure 2(a) shows the electron-phonon coupling at the vacuum level (E_V) with 14.7 meV phonon energy on 16 irreducible points of a $6\times6\times1$ grid in the SBZ. One would see that the electron-phonon coupling has minor value at every k point except for the $\bar{Y}$ point. The electron-phonon coupling spectrum as a function of the phonon energy should have a main peak around 14.7 meV because the step appears at this energy in the LPES result. As shown in Fig. 2(b), the spectrum at the $\bar{Y}$ point contains a peak around 14.7 meV. Thus, we have judged that the inelastic signal in the LPES result of Cu(110) originates from the indirect excitation process from the $\bar{Y}$ to the $\bar{\Gamma}$ point. Parenthetically, we note that the electronic states around E_F at the $\bar{Y}$ point on the real Cu(110) surface are available due to the spectral tail of the Shockley state, though the energy gap opens around E_F in the calculated band structure [Fig. 1(c)]. In other words, the step structure shown in Fig. 1(a) originates from the indirect transition from E_F level at the $\bar{Y}$ point where the electron is available due to the spectral tail of the Shockley states. It is reported that on the $\bar{\Gamma}$ Shockley state of the Cu(111) surface, the peak of which is located at around 420 meV below E_F, the spectral tail extends to E_F.[28,29] We believe that this is attributed to the presence of electrons around E_F at the $\bar{Y}$ point.

Figure 2(c) shows that, in addition to the $\bar{Y}$ point, several other k points also display strong electron-phonon coupling. However, on these k points, the electron-phonon coupling is weak around 14.7 meV, which indicates that the contribution of these k points for the inelastic process is minor. Let us investigate why the contribution from the $\bar{Y}$ point appears selectively in the spectra. One plausible explanation for this is the k-point dependency of the electronic dipole transition matrix element in Eq. (3), $\langle\psi_{q\alpha}|\vec{e}\cdot\vec{p}|\psi_{qv}\rangle$. In the elastic process, the final state of the dipole transition can be the free electron state in vacuum. Conversely, in the inelastic phonon-mediated process, the final state of the dipole transition in the inelastic phonon-mediated process should be an electronic state associated with Cu(110). The probability of the inelastic process is given by the product of the electron-phonon coupling and electronic dipole transition matrix element. As shown in Fig. 2(c), the electron-phonon coupling becomes large around the $\bar{X}$ (q4, q7), $\bar{Y}$ (q13), and $\bar{\Gamma}$ (q1, q5) points. Around the $\bar{X}$ point, the electronic dipole transition matrix element becomes small owing to the existence of the projected band gap [Fig. 1(b)]. Consequently, the inelastic transition process from the $\bar{X}$ point to the $\bar{\Gamma}$ point is prohibited. Although electronic states are available around E_V at the $\bar{\Gamma}$ point, the significant difference between the spatial distribution of charge at E_V and E_F [Fig. 3(a)] suppresses the inelastic process. (To highlight the difference, the product between the charge distribution around E_F and E_V at the $\bar{\Gamma}$ and $\bar{Y}$ point is also shown in Fig. 3.) The unoccupied electronic states around E_V at the $\bar{\Gamma}$ point are assigned to the image resonances.[30] Thus, the electronic states around E_V at the $\bar{\Gamma}$ point mainly distribute in the exterior of Cu. The electronic dipole transition matrix element is expected to be proportional to the overlap in the distribution of initial and final states. Therefore, the dipole excitation from E_F to the intrinsic electronic states of Cu(110), which is prerequisite to excite the phonon modes, is suppressed, and only the direct transition to the free electron band in vacuum is observed at the $\bar{\Gamma}$ point. In contrast, the charge distributions of the initial state (the Shockley surface state) and final state overlap in the interior of Cu at the $\bar{Y}$ point [Fig. 3(b)]. As a result, only the transition process from the $\bar{Y}$ point to the $\bar{\Gamma}$ point becomes dominant.

Now, we discuss the depth distribution of the phonon modes that appear in the inelastic LPES on Cu(110). An inspection of the phonon modes around 15 meV at the $\bar{Y}$ point (Fig. S1, Ref. 29) shows that the phonon modes polarized along the $[\bar{1}10]$ direction exhibit high density of states in the second and deeper layers, in spite of the low density of states in the topmost layer. Among them, we observe that four modes polarized along the $[\bar{1}10]$ direction with phonon energies of 13.45,

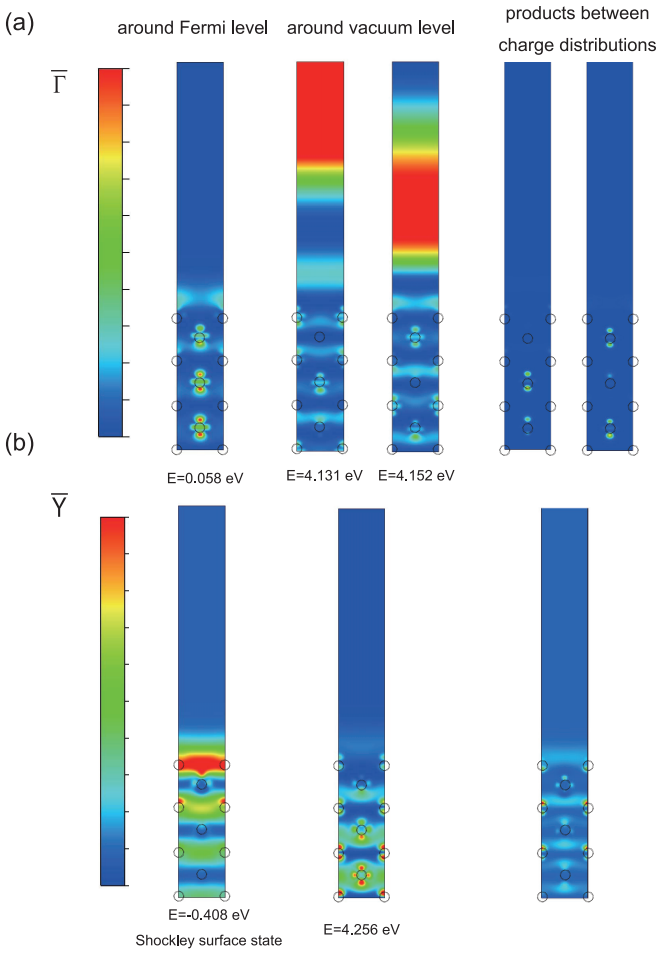

FIG. 3. (Color online) The charge distribution of electronic states around E_F and E_V at (a) the $\bar{\Gamma}$ and (b) the $\bar{Y}$ point, respectively. The product between the charge distribution around E_F and E_V is also shown. The color shows the summation of charge density projected onto the (001) surface. Red and blue indicate higher and lower values of the charge density, respectively. The dotted circle in each plot indicates the position of the Cu atoms. At the $\bar{Y}$ point, the electronic state closest to E_F is the Shockley surface state. Note that the "surface" state penetrates into the subsurface layer. The charge distribution of the Shockley surface state and bulk state at E_V overlap in the interior of Cu. In contrast, at the $\bar{\Gamma}$ point, the charge distribution of the electronic state near E_F and E_V exhibits minor overlap. These figures are rendered with VESTA.[34]

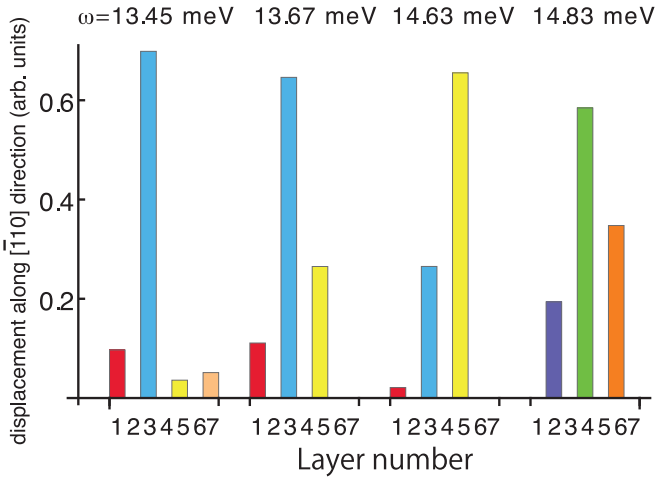

FIG. 4. (Color online) The distribution of atomic displacement from four phonon modes polarized along the [$\bar{1}$10] direction which couple with the photoelectron strongly at E_V at the $\bar{Y}$ point. ω is the phonon energy. The displacement in this figure is the absolute value of the projection onto the [$\bar{1}$10] direction. In all four modes, the atomic displacement is large in the subsurface region, which indicates that these modes are subsurface phonon modes.

13.67, 14.63, and 14.83 meV have large electron-phonon matrix elements and are the source of the main peak at the $\bar{Y}$ point in Fig. 2(b). As summarized in Fig. 4, these four modes are subsurface phonons. Incidentally, similar features are observed for the phonons polarized along the [100] and [001] directions. However, the electron-phonon couplings of these phonon modes that scatter the photoelectron from the $\bar{Y}$ to $\bar{\Gamma}$ point are smaller than those polarized along the [$\bar{1}$10] (not shown here); we do not discuss these modes further.

Subsurface phonons have recently been detected through helium atom scattering (HAS) experiments. We note here that the mechanism of the subsurface phonon excitation in HAS differs from that in LPES experiments, which is elucidated in the following. Subsurface phonon excitation in HAS is due to the strong charge oscillation at surfaces caused by the subsurface phonon mode,[31] which is totally different from the LPES experiments. In fact, the shear horizontal phonon modes that correspond to that polarized along the [$\bar{1}$10] direction in this study do not contribute significantly in HAS,[32] although they appeared in the LPES results. High resolution electron energy loss spectroscopy (HREELS)[33] experiments could be used to probe the subsurface phonon, because the electron in the inelastic impact regime may be scattered by the atom core oscillation in the first few layers. However, the 14.7 meV loss has not been observed in the HREELS spectra.[25] These results can be attributed to different underlying mechanisms. As we have demonstrated, the availability of the unoccupied states around E_V, which is not a prerequisite for HREELS, is of prime importance for the inelastic scattering of the photoelectron. It would be extremely interesting to extract the essences of the theory that predicts the inelastic photoemission by taking the difference between HREELS and LPES into consideration. Although the exact origin of the difference between HREELS and LPES is not completely clear, we have succeeded in demonstrating that the laser photoelectron excites the subsurface phonon; the current results also indicate that the LPES experiments provide a means for the characterization of subsurface phonons.

Before closing the discussion, let us compare the results in our previous[13] and current work. In the previous work, providing no theoretical calculations, we speculated the following inelastic process: The photoelectron is scattered to the $\bar{\Gamma}$ point by the interaction with the phonon which has the same wave number with photoelectron. Then, considering the electronic and phononic dispersion of bulk Cu, we concluded that the step structure arises from the coupling between the bulk T_1 phonon and photoelectron excited from the bulk electronic state at k_F. The current work supports the general mechanism of the inelastic photoemission process shown in the previous

work, however, our calculation results reveal that the origin of the inelastic step is the interaction between subsurface phonon and photoelectron excited from the surface Shockley state at $\bar{Y}$ point. On the other hand, the calculations show that the interaction between the bulk phonon and photoelectron is too weak to account for the inelastic component. We also point out that the selectivity of phonon modes in the inelastic process arises from the wave-number dependence of the electron-phonon coupling and the wave-function distribution. Such elucidations become first available by the detailed *ab initio* electron-phonon coupling calculation on the surface system, which is beyond the simple speculation based on the bulk properties. Thus, our understanding regarding the inelastic photoemission excited by the laser photon has been improved through the current work.

In summary, we have investigated the mechanism of inelastic processes in LPES on Cu(110) by conducting DFPT calculations and LPES experiments. We have succeeded in substantiating that the scattering of the low-energy photoelectron from the $\bar{Y}$ point to the $\bar{\Gamma}$ point mediated selectively by subsurface phonon modes during the photoemission process gives rise to the characteristic inelastic step structure in the spectra. The mechanism of subsurface detection in the LPES experiment differs from that in HAS and HREELS experiments, and this mechanism is expected to enable us to access subsurface phonons that have not been detected previously.

E.M. thanks H. Minamitani for technical support on programming. The calculations were performed by using the computer facilities of the Institute of Solid State Physics (ISSP Super Computer Center, University of Tokyo), and RIKEN Integrated Cluster of Clusters (RICC) facilities. This work was partially supported by Grants-in-Aid for Scientific Research (Nos. 24540332 and 25871114) from the Ministry of Education, Culture, Sports, Science and Technology, Japan (MEXT), and World Premier International Research Center Initiative (WPI), MEXT.

*eminamitani@riken.jp
†Corresponding author: ARAFUNE.Ryuichi@nims.go.jp

[1] *Very High Resolution Photoelectron Spectroscopy*, Lecture Notes in Physics, edited by S. Hüfner (Springer, Berlin Heidelberg, 2007).
[2] S. Hüfner, *Photoelectron Spectroscopy*, 3rd ed. (Springer, Berlin, Heidelbelg, New York, 2003).
[3] K. Kimura, J. Electron Spectrosc. Relat. Phenom. **100**, 273 (1999).
[4] M. Hengsberger, D. Purdie, P. Segovia, M. Garnier, and Y. Baer, Phys. Rev. Lett. **83**, 592 (1999).
[5] T. Valla, A. V. Fedorov, P. D. Johnson, and S. L. Hulbert, Phys. Rev. Lett. **83**, 2085 (1999).
[6] T. Valla, A. V. Fedorov, P. D. Johnson, B. O. Wells, S. L. Hulbert, Q. Li, G. D. Gu, and N. Koshizuka, Science **285**, 2110 (1999).
[7] P. Hofmann, C. Søndergaard, S. Agergaard, S. V. Hoffmann, J. E. Gayone, G. Zampieri, S. Lizzit, and A. Baraldi, Phys. Rev. B **66**, 245422 (2002).
[8] F. Reinert, B. Eltner, N. G., F. Forster, S. Schmidt, and S. Hüfner, Physica B: Condensed Matter **351**, 229 (2004).
[9] A. Eiguren, B. Hellsing, F. Reinert, G. Nicolay, E. V. Chulkov, V. M. Silkin, S. Hüfner, and P. M. Echenique, Phys. Rev. Lett. **88**, 066805 (2002).
[10] P. Echenique, R. Berndt, E. Chulkov, T. Fauster, A. Goldmann, and U. Höfer, Surf. Sci. Rep. **52**, 219 (2004).
[11] P. Hofmann, I. Y. Sklyadneva, E. D. L. Rienks, and E. V. Chulkov, New J. Phys. **11**, 125005 (2009).
[12] R. Arafune, K. Hayashi, S. Ueda, Y. Uehara, and S. Ushioda, Phys. Rev. Lett. **95**, 207601 (2005).
[13] R. Arafune, M. Q. Yamamoto, N. Takagi, and M. Kawai, Phys. Rev. B **80**, 073407 (2009).
[14] In this experiment, the excitation light is an ultraviolet pulse (pulse width 2 ps) produced by the frequency tripling of Ti: Sapphire laser light in nonlinear crystals. The p-polarized light was incident at 54° measured from the surface normal. The emitted photoelectrons were measured in the normal emission geometry with an acceptance angle of 1° and an energy resolution of 4 meV.
[15] K. Ishizaka, R. Eguchi, S. Tsuda, A. Chainani, T. Yokoya, T. Kiss, T. Shimojima, T. Togashi, S. Watanabe, C.-T. Chen, Y. Takano, M. Nagao, I. Sakaguchi, T. Takenouchi, H. Kawarada, and S. Shin, Phys. Rev. Lett. **100**, 166402 (2008).
[16] C. Bandis and B. B. Pate, Phys. Rev. Lett. **74**, 777 (1995).
[17] S. Baroni, S. de Gironcoli, A. Dal Corso, and P. Giannozzi, Rev. Mod. Phys. **73**, 515 (2001).
[18] *Ab initio* calculations at the level of the generalized gradient approximation (GGA) with the Perdew-Burke-Ernzerhof (PBE) functional[35] are performed using the QUANTUM-ESPRESSO distribution.[36] We modeled the surface with the fully relaxed 13-layer Cu(110) slab with a ∼28 Å thick vacuum along the surface normal. The unit cell and the corresponding SBZ are shown in Fig. 1(b). An ultrasoft pseudopotential generated with the Rappe, Rabe, Kaxiras, and Joannopoulos (RRKJ3) scheme (Ref. 37) is used for Cu. The expansion of the plane-wave basis set is restricted by a kinetic energy cutoff of 35 Ry. For the phonon calculations, we set the charge density cutoff to 400 Ry. A $12 \times 12 \times 1$ Monkhorst-Pack grid[38] without an offset is used for the ionic relaxation and self-consistent electronic structure calculations. A finer $24 \times 24 \times 1$ grid is used for the integration of the first SBZ in the electron-phonon coupling calculations. The phonon dispersion and the electron-phonon coupling are calculated on the uniform $6 \times 6 \times 1$ grid in the SBZ, which includes the high symmetry points: $\bar{\Gamma}$, $\bar{X}$, $\bar{S}$, and $\bar{Y}$.
[19] J. Harl, G. Kresse, L. D. Sun, M. Hohage, and P. Zeppenfeld, Phys. Rev. B **76**, 035436 (2007).
[20] P. Straube, F. Pforte, T. Michalke, K. Berge, A. Gerlach, and A. Goldmann, Phys. Rev. B **61**, 14072 (2000).
[21] A. Baldereschi, S. Baroni, and R. Resta, Phys. Rev. Lett. **61**, 734 (1988).
[22] R. Arafune, K. Hayashi, S. Ueda, and S. Ushioda, Phys. Rev. Lett. **92**, 247601 (2004).
[23] C. J. Fall, N. Binggeli, and A. Baldereschi, J. Phys.: Condens. Matter **11**, 2689 (1999).
[24] N. E. Singh-Miller and N. Marzari, Phys. Rev. B **80**, 235407 (2009).
[25] R. Heid and K.-P. Bohnen, Phys. Rep. **387**, 151 (2003).

[26]P. Zeppenfeld, K. Kern, R. David, K. Kuhnke, and G. Comsa, Phys. Rev. B **38**, 12329 (1988).
[27]G. Grosso and G. P. Parravinici, *Solid State Physics* (Academic Press, New York, 2000) .
[28]R. Arafune, K. Hayashi, S. Ueda, Y. Uehara, and S. Ushioda, J. Phys. Soc. Jpn. **76**, 044604 (2007).
[29]See Supplemental Material at http://link.aps.org/supplemental/10.1103/PhysRevB.88.224301 for the photoemission spectrum of the surface Shockley state on Cu(111) and k-resolved phonon density of states projected to [001], [1$\bar{1}$0], and [100] direction.
[30]Y. Sonoda, Phys. Rev. B **83**, 245410 (2011).
[31]V. Chis, B. Hellsing, G. Benedek, M. Bernasconi, E. V. Chulkov, and J. P. Toennies, Phys. Rev. Lett. **101**, 206102 (2008).
[32]I. Y. Sklyadneva, G. Benedek, E. V. Chulkov, P. M. Echenique, R. Heid, K.-P. Bohnen, and J. P. Toennies, Phys. Rev. Lett. **107**, 095502 (2011).
[33]H. Ibach and D. L. Mills, *Electron Energy Loss Spectroscopy and Surface Vibrations* (Academic, New York, 1982) .
[34]K. Momma and F. Izumi, J. Appl. Crystallogr. **41**, 653 (2008).
[35]J. P. Perdew, K. Burke, and M. Ernzerhof, Phys. Rev. Lett. **77**, 3865 (1996).
[36]P. Giannozzi, S. Baroni, N. Bonini, M. Calandra, R. Car, C. Cavazzoni, D. Ceresoli, G. L. Chiarotti, M. Cococcioni, I. Dabo, A. D. Corso, S. de Gironcoli, S. Fabris, G. Fratesi, R. Gebauer, U. Gerstmann, C. Gougoussis, A. Kokalj, M. Lazzeri, L. Martin-Samos, N. Marzari, F. Mauri, R. Mazzarello, S. Paolini, A. Pasquarello, L. Paulatto, C. Sbraccia, S. Scandolo, G. Sclauzero, A. P. Seitsonen, A. Smogunov, P. Umari, and R. M. Wentzcovitch, J. Phys.: Condens. Matter **21**, 395502 (2009).
[37]A. M. Rappe, K. M. Rabe, E. Kaxiras, and J. D. Joannopoulos, Phys. Rev. B **41**, 1227 (1990).
[38]H. J. Monkhorst and J. D. Pack, Phys. Rev. B **13**, 5188 (1976).